

# Development of a Two-Stage Radial Inflow Turbine for a Mini-ORC

Martin HEYLEN<sup>1,2,3\*</sup>, Vincent LEMORT<sup>2</sup>, Michel DELANAYE<sup>1</sup>, Koen HILLEWAERT<sup>3</sup>

<sup>1</sup> Mitis SA

5, rue des Chasseurs Ardennais – 4031 Angleur

<sup>2</sup> Laboratoire de Thermodynamique – Université de Liège

17 Bât B49, Allée de la Découverte – 4000 Liège

<sup>3</sup> Design of Turbomachines – Université de Liège

9 Bât B52/3, Allée de la Découverte – 4000 Liège

\*(Corresponding author : martin.heylen@mitis.be)

**Résumé** - Ce travail est centré sur la construction d'un modèle 0-D de conception de roue turbine radial pour des fluides non idéaux. Ce modèle est appliqué au cas d'un cycle ORC de  $10kWe$  à deux étages d'expansion. Le point de fonctionnement du système ainsi que le fluide de travail sont choisis sur base des contraintes propres aux turbomachines. Enfin, une vérification CFD sur base des roues conçues est réalisée afin de valider le modèle, et de vérifier certaines caractéristiques de l'écoulement prédites sur base du modèle 0-D.

## Nomenclature

$V$  absolute velocity, m/s  
 $W$  relative velocity, m/s  
 $U$  blade tip velocity, m/s  
 $C_m$  meridional velocity, m/s  
 $Q$  volumetric flow rate, m<sup>3</sup>/s  
 $Ma$  Mach Number

$T$  temperature, K  
 $P$  pressure, Pa or bar  
 $h$  enthalpy, J/kg  
 $c$  speed of sound, m/s

$r$  radius, mm  
 $h$  tip blade height, mm  
 $A$  cross section area, mm<sup>2</sup>  
 $\Delta z$  axial length, mm

### adimensional parameters

$N_s$  specific speed  
 $C_s$  spouting velocity  
 $V_{ts}$  velocity ratio  
 $C_{m,ratio}$  meridional speed ratio

### Greeks Symbols

$\alpha$  angle of attack, deg  
 $\beta$  incidence angle, deg  
 $\eta$  isentropic efficiency, %

$\omega$  rotational speed, rad/s  
 $\rho$  density, kg/m<sup>3</sup>

### abbreviation

CHP Combined Heat and Power  
RIT Radial Inflow Turbine  
CFD Computational Fluid Dynamics  
ORC Organic Rankine Cycle  
PS Pressure Side  
SS Suction Side

### subscript

4 rotor Inlet  
5 rotor Outlet  
 $h$  hub  
 $sh$  shroud

$\theta$  tangential  
 $m$  meridional

$evap$  evaporator  
 $cond$  condenser

$t$  total  
 $s$  static  
 $id$  isentropic total to static

## 1. Introduction

Nowadays, the decarbonization of energy systems is targeted to strive for the zero-emission target. Considering a gas turbine based **Combined Heat and Power** system (CHP), this objective is pursued through the use of biofuel and by improving system efficiency; or more precisely by improving the efficiency of the subcomponent that ensures the transfer of the mechanical energy. It mainly consists of a centrifugal compressor and a **Radial Inflow Turbine (RIT)** positioned on the same shaft, together with the generator. Additionally, the wasted heat can be converted into useful energy by coupling the CHP with bottoming cycles. Among the possibilities, **Organic Rankine Cycles (ORC)** are suited systems for low-temperature heat recovery [1]. Another RIT can be integrated into ORC as an expansion device.

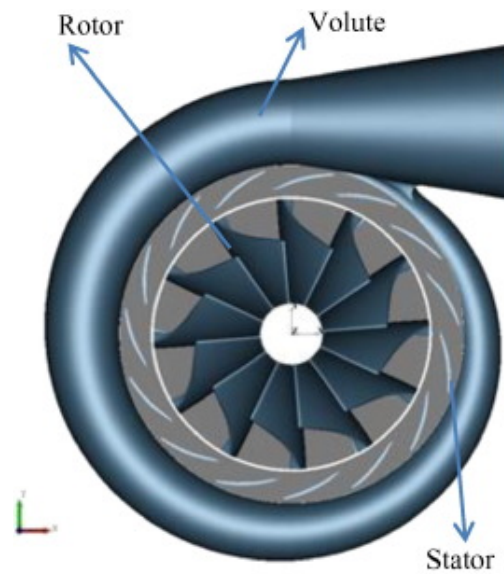


Figure 1 : *Volute, nozzle (Stator), and radial turbine (Rotor) schematic [2]*

The scientific literature review has shown that many developments have been brought by the community to provide design tools for the radial turbine and the associated volute (Figure 1). An analytical method to design and predict the performance of the radial turbine has been proposed. The model provides the rotor geometry for any operating conditions [3]. A guideline for preliminary sizing of the rotor has been proposed to provide empirical correlations to assess the losses in the turbine [4]. This approach has been applied for the design of a 5kWe micro radial turboexpander ORC using R134a as working fluid [5]. They optimized the rotor shape based on the blade loading and flow distribution in the meridional plane. A two stage radial inflow turbine integrated into a 50kWe ORC has been investigated [6].

This paper introduces a design method for radial inflow turbines, using detailed thermodynamic tables for the gas. The application in this publication is the development of two radial inflow turbine stages for a 10kWe ORC. This small power has not been covered in the current literature for two stage turbine machines.

This paper will present a preliminary validation of the model through CFD analysis. the paper will discuss the current limitations of the model with potential future improvements.

## 2. Radial inflow turbine design model ([4], [3])

The present 0-D model provides a tool to design a radial inflow turbine. As these devices are designed to work with gas, the working fluid must be gaseous during the complete expansion.

The model is developed within the Excel framework and relies on the thermodynamic library CoolProp [7] for the fluid properties. It calculates the velocity triangle (depicted in Figure 2) at the rotor inlet and outlet to describe the flow velocity at these strategic points.

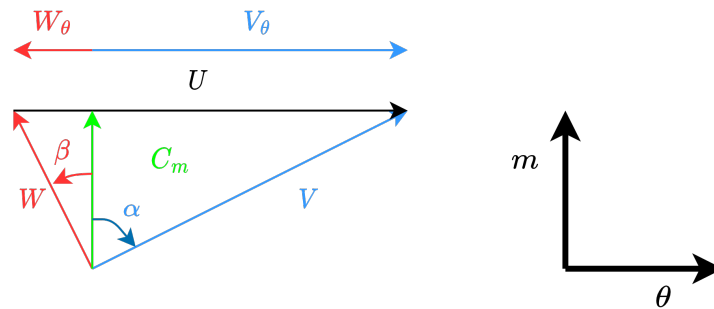


Figure 2 : Velocity Triangle

The velocity triangle is composed of 4 velocity vectors, namely

1. the absolute velocity  $V$ , the velocity seen by a non-rotating (or stationary) frame
2. the relative velocity  $W$  seen by the rotating frame attached to the rotor
3. the blade rotation velocity  $U$ , which is the rotating velocity of the blade
4. the meridional velocity  $C_m$ , which is the flow velocity projected on the (local) meridional axis  $m$  (Figure 3)

Moreover, the absolute and relative angles  $\alpha$  and  $\beta$  are respectively defined between the meridional velocity and the absolute and relative velocity components respectively in the tangential direction.

Figure 3 illustrates a meridional cut of the radial turbine rotor. It contains most of the geometrical parameters obtained through the design.

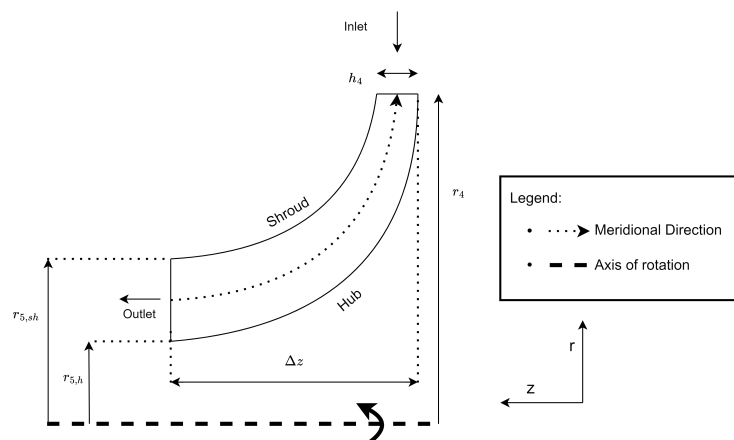


Figure 3 : Radial turbine meridional plane. 4 :inlet, 5 :outlet; h :hub, sh :shroud.

## 2.1. Specific Speed

During the design, the model computes several non-dimensional quantities. The first parameter is the specific speed  $N_s$  (Equation 1). The specific speed for any operating condition is the non-dimensional number

$$N_s = \frac{\omega \sqrt{Q_5}}{\Delta h_{id}^{0.75}} \quad (1)$$

where  $\omega$  is the rotational speed,  $Q_5$  the volumetric flow at the rotor exit, and  $\Delta h_{id}$  is the isentropic drop of enthalpy generated by the "expansion from the stage inlet total conditions to the rotor outlet static conditions" [3].

For a radial inflow turbine, the specific speed at the design point must be within the range  $N_s \in [0.45, 0.75]$  [3, 8]. This condition will insure a certain stability of the rotor during operations.

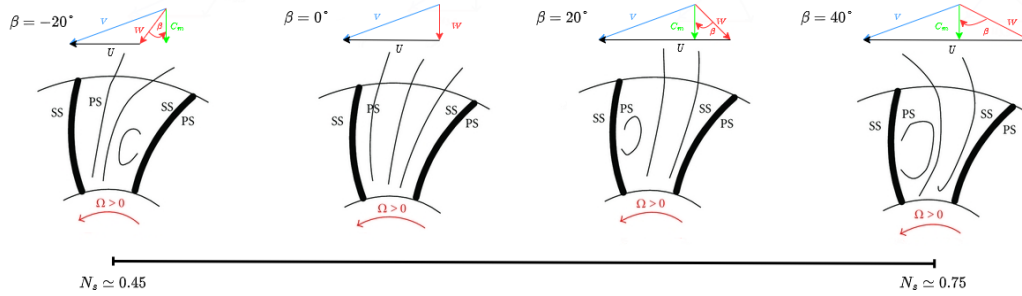


Figure 4 : Variation of the inlet incidence angle versus the specific speed of the rotor at various operating points for a given design [8].

$N_s$  : Specific Speed; PS : Pressure Side, SS : Suction Side

Figure 4 illustrates the flow physics within the rotor for different incidence flow angles [8]. Considering a rotating blade, a zone of pressure and suction will be generated on each blade side. The schematic depicts that there is a link between the specific speed  $N_s$  associated to the operating point and the incidence angle  $\beta_4$ .

As indicated, a reverse flow area is observed when the specific speed tends to be too small or too large. Therefore, it is required to maintain the specific speed within the previously mentioned boundaries. In the literature, it is recommended to design the turbine so that the inlet incidence angle  $\beta_4$  is close to  $0^\circ$  to minimize the recirculating zone. This is emphasized in Figure 4

## 2.2. Inlet Velocity Triangle

The design of the radial inflow turbine start by calculating the inlet velocity triangle. First is defined the spouting velocity  $C_s$  (Equation 2), defined as being the velocity associated with the enthalpy drop  $\Delta h_{id}$ , is also computed :

$$C_s = \sqrt{2\Delta h_{id}} \quad (2)$$

The spouting velocity, multiplied by the total to static velocity ratio  $V_{ts}$  defined in Equation 3, allows the assessment of the rotor tip speed rotating speed  $U_4$  (Equation 4) :

$$V_{ts} = 0.737N_s^{0.2} \quad (3)$$

$$U_4 = C_s \times V_{ts} = \omega \times r_4 \quad (4)$$

Regarding total and static quantities, a static quantity (pressure, temperature,...) corresponds to the properties of the medium where the flow velocity is zero. When considering a total property, the influence of the flow velocity is included during the calculation.

Continuing with the assessment of the inlet velocity triangle, the absolute velocity's tangential component is computed from Equation 5 :

$$C_{\theta,4} = \frac{U_4 \times \eta_{ts}}{2V_{ts}^2} \quad (5)$$

where  $\eta_{ts}$  is the total to static isentropic efficiency estimated through the Equation 6 :

$$\eta_{ts} = 0.87 - 1.07(N_s - 0.55)^2 - 0.5(N_s - 0.55)^3 \quad (6)$$

Lastly, the rotor angle of attack  $\alpha_4$  must be defined. This angle has been found to be optimal when following Equation 7 [4].

$$\alpha_4 = 10.8 + 14.2N_s^2 \quad (7)$$

Then, the remaining inlet velocity triangle is obtained through trigonometry calculation.

### 2.3. Rotor Inlet Design

The geometrical parameters to describe the rotor inlet (station 4) are the outer radius  $r_4$ , the blade tip height  $h_4$ , and the blade angle. It is a good practice to set radial the inlet rotor blade [9]. Considering the tip height  $h_4$ , it is computed through Equation 8

$$A_4 = \frac{\dot{m}}{\rho_{s,4} \times C_{m,4}} = 2\pi \times r_4 \times h_4 \quad (8)$$

where  $\rho_{s,4}$  is the density of the inlet flow calculated based on the static conditions.

### 2.4. Rotor Outlet Design

With the rotor inlet design being established, the outlet velocity triangle can be constructed. First the outlet meridional velocity  $C_{m,5}$  is obtained through the meridional velocity ratio  $C_{m,ratio}$  defined in Equation 9 [3] :

$$C_{m,ratio} = \frac{C_{m,5}}{C_{m,4}} = 1 + 5 \times (h/r_4)^2 \quad (9)$$

At the outlet, it is assumed that the tangential component of the absolute velocity  $V_{\theta,5}$  is zero. This hypothesis is justified as this component will only dissipate the energy through the induced swirl.

At the outlet of the turbine, the radius at the hub  $r_{h,5}$  is given by Equation 10 [10] :

$$r_{h,5} = 0.185r_4 \quad (10)$$

From this point, it is possible to assess the radius at the shroud  $r_{sh,5}$  and the rotating velocities  $U_{h,5}$  and  $U_{sh,5}$ . Once the velocity triangles at the hub and shroud are computed, the blade angles at the hub and shroud are respectively associated with the relative angle  $\beta_{h,5}$  and  $\beta_{sh,5}$ .

### 3. Case study : ORC

In this work, a simple design model of a radial inflow turbine has been developed. the application of the model is the integration of high-speed turbines within two expansion stages Organic Rankine Cycle (ORC) ( Figure 5) producing an electrical power of  $10kW_e$ .

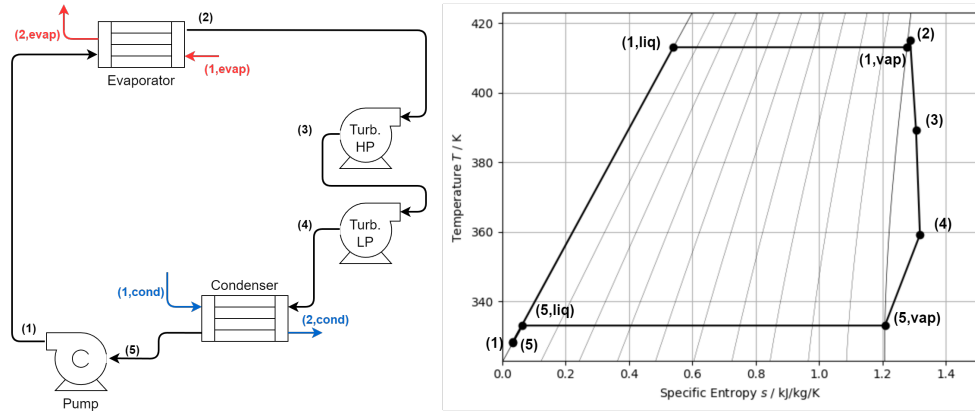


Figure 5 : Organic Rankine Cycle schematic - TS diagram for Cyclopentane

#### 3.1. Working Fluid Selection

The speed of sound  $c$  of organic fluids is typically low. Therefore, attention must be paid to the Mach number  $Ma$  which should not go beyond  $Ma = 1$  if supersonic turbine behavior is unintended.

Working Fluid	R123	R1233zd	R245fa	novec649	cyclopentane
Speed of sound [m/s]	136	149	149	76	196
Density [kg/m <sup>3</sup> ]	42	35	35	103	20
Crit. Temperature [°C]	184	166	154	169	239

Table 1 : Working Fluid comparison for a temperature  $T = 130^\circ C$  and a pressure  $P = 8 \text{ bar}$  [7]

Table 1 shows that the speed of sound has a link with the fluid density. Based on the rotational velocity constraint imposed, a low-density fluid must be selected to design a high-speed radial turbine for ORC. From the selected fluids, cyclopentane is the best candidate for the design of a high-speed radial turbine without lying in the supersonic zone.

#### 3.2. Operating Point Selection

When defining the nominal operating point of the ORC, the condensation and evaporation temperatures ( $T_{cond}$  and  $T_{evap}$ , respectively) have to be defined. Regarding the former temperature, it has been set at  $60^\circ C$ . This temperature is such that it is compatible with conventional heat emitters in buildings.

The evaporating temperature  $T_{evap}$  has been imposed by considering the generator magnet's curie temperature. In this paper, it has been selected a temperature  $T_{evap} = 130^\circ C$ .

Regarding the mass flow rate, it has been selected to reach the electrical power generation of  $10kWe$  at the nominal operating point. Table 2 provides the nominal operating point of each radial turbine.

	Inlet Temp.	Total Inlet Pres.	Total Inlet Pres.	TT Expansion Ratio	Mass Flow Rate	Working Fluid
HP Turbine	131.85°C	7.87 bar	7.87 bar	2.567	165 g/s	Cyclopentane
LP Turbine	104.85°C	1.42 bar	1.42 bar	2.163	165 g/s	Cyclopentane

Table 2 : *Radial Turbine Operating Condition.*

### 3.3. CFD Validation

This last section is providing a validation of the design model through CFD. In the scope of this paper, the model will be validated with the design of the high-pressure radial turbine. The software **CFX** from Ansys will provide an accurate point of comparison for the 0-D model. To integrate the design, a bridge has been developed in Python [11] to generate a blade design file readable by the computational fluid dynamic software.

The comparison of the performance has been done by assessing the nominal operating point in **CFX**. As a reminder, the inlet condition are 131°C and 7.87 bar with a mass flow rate of 165 g/s. The formulae used in the 0-D model predicted that the flow angle of attack and rotor isentropic efficiency of 73.73° and 86.5% respectively. These information has been compared in Table 3. It can be observed that the deviation of the 0-D model is relatively small.

<b>HP Turbine</b>	angle of attack [°] $\alpha_4$	Total to Static Isentropic Efficiency [%]	Total to Total Expansion Ratio
0-D Model	73.73°	86.5%	2.567
CFD	73.73°	85.5%	2.571
Delta	0%	1.15%	0.15%

Table 3 : *0-D model vs CFD : Performance Comparison.*

Then, it is verified the prediction of the 0-D model regarding the physics of the flow. The model estimated a value of  $\beta_4 = -7.5$  for the incidence angle. Considering Figure 4, a small recirculation should occur at the suction zone. After the Computation of the CFD, Figure 6 illustrates how the flow is distributed through the rotor passage.

As highlighted in the diagram, a small reverse flow occurs at the beginning of the blade's suction side (SS). This behavior is in line with the theoretical concept as the relative flow angle at the rotor entrance is quasi-radial.

## 4. Conclusion

This paper presented a model to design a radial inflow turbine for real gas. In the scope of this paper, only the development regarding the geometrical calculation of the entrance and exit of the rotor has been described. As the CFD comparison shows, the 0-D model is relatively accurate regarding the predicted performance and flow distribution within the radial turbine rotor passage.

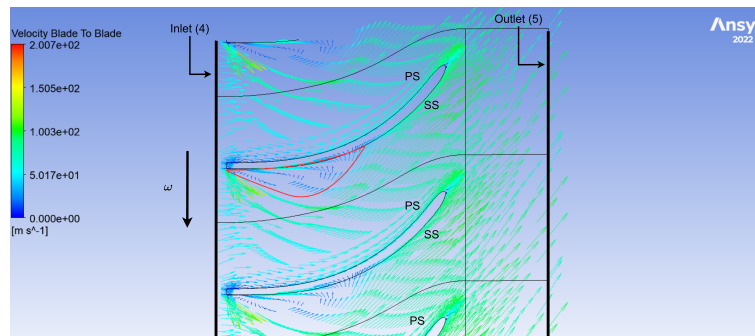


Figure 6 : Flow pattern through the Rotor passage (HP Turbine)

It has been demonstrated in this work that small ORC turbines ( $10\text{kWe}$ ) are providing good performances and may be pertinent for the application. Further developments have to be made to the model. First, the implementation of the volute design and performance prediction is missing. Moreover, loss correlations are not yet taken into account during the design phase.

## Références

- [1] S. Quoilin, “Sustainable energy conversion through the use of organic rankine cycles for waste heat recovery and solar applications.” phdthesis, Faculty of Applied Science of the University of Liège, Oct. 2011. [Online]. Available : <https://hdl.handle.net/2268/96436>
- [2] M. Azimian and H.-J. Bart, “Computational analysis of erosion in a radial inflow steam turbine,” *Engineering Failure Analysis*, vol. 64, pp. 26–43, jun 2016.
- [3] A. K. Noughabi and S. Sammak, “Detailed design and aerodynamic performance analysis of a radial-inflow turbine,” *Applied Sciences*, vol. 8, no. 11, p. 2207, nov 2018.
- [4] D. Fiaschi, G. Manfrida, and F. Maraschiello, “Design and performance prediction of radial ORC turboexpanders,” *Applied Energy*, vol. 138, pp. 517–532, jan 2015.
- [5] D. Fiaschi, G. Innocenti, G. Manfrida, and F. Maraschiello, “Design of micro radial turboexpanders for ORC power cycles : From 0d to 3d,” *Applied Thermal Engineering*, vol. 99, pp. 402–410, apr 2016.
- [6] A. Giovannelli, E. M. Archilei, and C. Salvini, “Two-stage radial turbine for a small waste heat recovery organic rankine cycle (ORC) plant,” *Energies*, vol. 13, no. 5, p. 1054, feb 2020.
- [7] I. H. Bell, J. Wronski, S. Quoilin, and V. Lemort, “Pure and pseudo-pure fluid thermophysical property evaluation and the open-source thermophysical property library coolprop,” *Industrial & Engineering Chemistry Research*, vol. 53, no. 6, pp. 2498–2508, 2014. [Online]. Available : <http://pubs.acs.org/doi/abs/10.1021/ie4033999>
- [8] Lüddecke, B. . Filsinger, and J. Dietmar & Ehrhard, “On mixed flow turbines for automotive turbocharger applications,” *International Journal of Rotating Machinery*, 2012.
- [9] A. Bayomi and Nazih, “Radial turbine design process,” *ISESCO Journal of Science and Technology*, 2015.
- [10] R. H. Aungier, “Turbine aerodynamics : Axial-flow and radial-flow turbine design and analysis,” 2006.
- [11] G. Van Rossum and F. L. Drake Jr, *Python reference manual*. Centrum voor Wiskunde en Informatica Amsterdam, 1995.